

Enhancing solar cells with localized plasmons in nanovoids

N. N. Lal,¹ B. F. Soares,¹ J. K. Sinha,² F. Huang,¹ S. Mahajan,¹
P. N. Bartlett,² N. C. Greenham,¹ and J. J. Baumberg^{1,*}

¹*Cavendish Laboratory, University of Cambridge, CB3 0HE, United Kingdom*

²*School of Chemistry, University of Southampton, Southampton, SO17 1BJ, United Kingdom*

[*jjb12@cam.ac.uk](mailto:jjb12@cam.ac.uk)

Abstract: Localized plasmon resonances of spherical nanovoid arrays strongly enhance solar cell performance by a factor of 3.5 in external quantum efficiency at plasmonic resonances, and a four-fold enhancement in overall power conversion efficiency. Large area substrates of silver nanovoids are electrochemically templated through self-assembled colloidal spheres and organic solar cells fabricated on top. Our design represents a new class of plasmonic photovoltaic enhancement: that of localized plasmon-enhanced absorption within nanovoid structures. Angularly-resolved spectra demonstrate strong localized Mie plasmon modes within the nanovoids. Theoretical modelling shows varied spatial dependence of light intensity within the void region suggesting a first possible route towards Third Generation plasmonic photovoltaics.

© 2011 Optical Society of America

OCIS codes: (240.6680) Surface plasmons; (310.6860) Thin films, optical properties; (040.5350) Photovoltaics.

References and links

1. V. E. Ferry, J. N. Munday, and H. A. Atwater, "Design considerations for plasmonic photovoltaics," *Adv. Mater.* **22**, 4794–4808 (2010).
2. H. A. Atwater and A. Polman, "Plasmonics for improved photovoltaic devices," *Nat. Mater.* **9**, 205–213 (2010).
3. K. Catchpole and A. Polman, "Plasmonic solar cells," *Opt. Express* **16**, 21793–21800 (2008).
4. V. Ferry, M. Verschuuren, H. Li, E. Verhagen, B. Hongbo, R. Walters, R. E. I. Schropp, H. A. Atwater, and A. Polman, "Light trapping in ultrathin plasmonic solar cells," *Opt. Express* **18**, 237–245 (2010).
5. J. Zhu, C.-M. Hsu, Z. Yu, S. Fan, and Y. Cui, "Nanodome solar cells with efficient light management and self-cleaning," *Nano Lett.* **10**, 1979–1984 (2010).
6. A. J. Morfa, K. L. Rowlen, T. H. Reilly, M. J. Romero, and J. van De Lagemaat, "Plasmon-enhanced solar energy conversion in organic bulk heterojunction photovoltaics," *Appl. Phys. Lett.* **92**, 013504 (2008).
7. J. N. Munday and H. A. Atwater, "Large integrated absorption enhancement in plasmonic solar cells by combining metallic gratings and antireflection coatings," *Nano Lett.* (2010), DOI: 10.1021/nl101875t.
8. K. Soderstrom, F. Haug, J. Escarre, O. Cubero, and C. Ballif, "Photocurrent increase in n-i-p thin film silicon solar cells by guided mode excitation via grating coupler," *Appl. Phys. Lett.* **96**, 213508 (2010).
9. C. Chao, C. Wang, and J. Chang, "Spatial distribution of absorption in plasmonic thin film solar cells," *Opt. Express* **18**, 11763–11771 (2010).
10. R. A. Pala, J. White, E. Barnard, J. Liu, and M. L. Brongersma, "Design of plasmonic thin-film solar cells with broadband absorption enhancements," *Adv. Mater.* **21**, 3504–3509 (2009).
11. N. C. Lindquist, W. A. Luhman, S.-H. Oh, and R. J. Holmes, "Plasmonic nanocavity arrays for enhanced efficiency in organic photovoltaic cells," *Appl. Phys. Lett.* **93**, 123308 (2008).
12. K. Tvingstedt, N.-K. Persson, O. Inganas, A. Rahachou, and I. V. Zozoulenko, "Surface plasmon increase absorption in polymer photovoltaic cells," *Appl. Phys. Lett.* **91**, 113514 (2007).
13. J. W. Menezes, J. Ferreira, M. J. L. Santos, L. Cescato, and A. G. Brolo, "Large-area fabrication of periodic arrays of nanoholes in metal films and their application in biosensing and plasmonic-enhanced photovoltaics," *Adv. Func. Mater.* **20**, 3918–3924 (2010).

14. W. Bai, Q. Gan, G. Song, L. Chen, Z. Kafafi, and F. Bartoli, "Broadband short-range surface plasmon structures for absorption enhancement in organic photovoltaics," *Opt. Express* **18**, 620–630 (2010).
15. V. E. Ferry, M. A. Verschuuren, H. B. T. Li, R. E. I. Schropp, H. A. Atwater, and A. Polman, "Improved red-response in thin film a-Si:H solar cells with soft-imprinted plasmonic back reflectors," *Appl. Phys. Lett.* **95**, 183503 (2009).
16. T. H. Reilly, J. van De Lagemaat, R. C. Tenent, A. J. Morfa, and K. L. Rowlen, "Surface-plasmon enhanced transparent electrodes in organic photovoltaics," *Appl. Phys. Lett.* **92**, 243304 (2008).
17. R. M. Cole, J. J. Baumberg, F. J. Garcia De Abajo, S. Mahajan, M. Abdelsalam, and P. N. Bartlett, "Understanding plasmons in nanoscale voids," *Nano Lett.* **7**, 2094–2100 (2007).
18. T. Kelf, Y. Sugawara, R. Cole, J. Baumberg, M. Abdelsalam, S. Cintra, S. Mahajan, A. Russell, and P. Bartlett, "Localized and delocalized plasmons in metallic nanovoids," *Phys. Rev. B* **74**, 1–12 (2006).
19. P. N. Saeta, V. E. Ferry, D. Pacifici, J. N. Munday, and H. A. Atwater, "How much can guided modes enhance absorption in thin solar cells?" *Opt. Express* **17**, 20975–20990 (2009).
20. S. Mahajan, R. M. Cole, B. F. Soares, S. H. Pelfrey, A. E. Russell, J. J. Baumberg, and P. N. Bartlett, "Relating SERS intensity to specific plasmon modes on sphere segment void surfaces," *J. Phys. Chem. C* **113**, 9284–9289 (2009).
21. J. Baumberg, "Plasmon-enhanced low-cost photovoltaics," EU Patent 2047521 (2007).
22. F. J. Beck, S. Mokkaapati, A. Polman, and K. R. Catchpole, "Asymmetry in photocurrent enhancement by plasmonic nanoparticle arrays located on the front or on the rear of solar cells," *Appl. Phys. Lett.* **96**, 033113 (2010).
23. M. E. Abdelsalam, P. N. Bartlett, T. Kelf, and J. J. Baumberg, "Wetting of regularly structured gold surfaces," *Langmuir* **21**, 1753–1757 (2005).
24. T. V. Teperik, F. J. Garcia de Abajo, A. G. Borisov, M. Abdelsalam, P. N. Bartlett, Y. Sugawara, and J. J. Baumberg, "Omnidirectional absorption in nanostructured metal surfaces," *Nat. Photonics* **2**, 299–301 (2008).
25. P. N. Bartlett, J. J. Baumberg, P. R. Birkin, M. A. Ghanem, and M. C. Netti, "Highly ordered macroporous gold and platinum films formed by electrochemical deposition through templates assembled from submicron diameter monodisperse polystyrene spheres," *Chem. Mater.* **14**, 2199–2208 (2002).
26. F. Garcia De Abajo and A. Howie, "Relativistic electron energy loss and electron-induced photon emission in inhomogeneous dielectrics," *Phys. Rev. Lett.* **80**, 5180–5183 (1998).
27. H. Hoppe, S. Shokhovets, and G. Gobsch, "Inverse relation between photocurrent and absorption layer thickness in polymer solar cells," *Phys. Status Solidi (RRL)* **1**, R40–R42 (2007).
28. L. A. Pettersson, S. Ghosh, and O. Inganas, "Optical anisotropy in thin films of poly(3,4-ethylenedioxythiophene)poly(4-styrenesulfonate)," *Org. Electron.* **3**, 143–148 (2002).
29. E. D. Palik, *Handbook of Optical Constants of Solids* (Academic Press, 1985).
30. Y. Kim, S. Cook, S. M. Tuladhar, S. A. Choulis, J. Nelson, J. R. Durrant, D. D. C. Bradley, M. Giles, I. McCulloch, C.-S. Ha, and M. Ree, "A strong regioregularity effect in self-organizing conjugated polymer films and high-efficiency polythiophene:fullerene solar cells," *Nat. Mater.* **5**, 197–203 (2006).

1. Introduction

To increase the efficiencies of the next generation of solar cells, researchers are turning their attention to plasmonics as a way of enhancing light-absorption in thin-film materials [1–3]. To date, plasmonic enhancement for photovoltaics has mainly focused on Mie scattering resonances of noble metal nanoparticles and plasmonic coupling into waveguide modes via nanostructured top and rear contacts of solar cells [4–16]. Here we demonstrate a new class of plasmonic photovoltaic enhancement: that of localized-plasmon enhanced absorption *within* nanovoid structures. Our approach is to exploit strong localized plasmonic resonances of spherical nanocavities grown via scalable self-assembly [17, 18] to enhance light absorption in photoactive materials. We report first organic cells fabricated inside these nanostructures that reproducibly yield an enhancement factor of 3.5 in external quantum efficiency at plasmonic resonances, and a four-fold enhancement in overall power conversion efficiency. While the absolute efficiencies of these plasmonic photovoltaics are not yet high enough, we are able here to clearly demonstrate the significant plasmonic enhancements achievable with this concept.

Texturing noble metals on the nanoscale provides the opportunity to control surface plasmon resonances at metal-dielectric interfaces. While the inclusion of nanostructured metals in solar cells presents challenges of fabrication, metallic absorption and resistance losses, choosing the right structure enables an enhancement in overall device performance.

The Mie resonances of noble metal nanoparticles have been applied to solar cells of varied

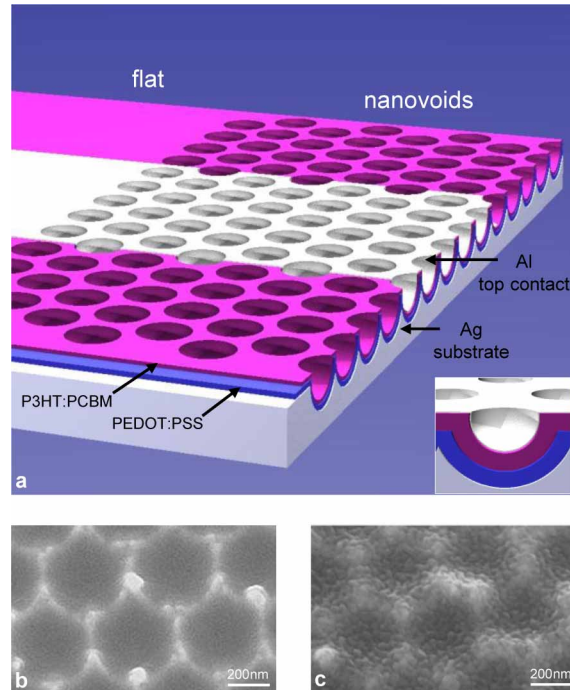


Fig. 1. (a) Schematic representation of the cell geometry with separate flat and nanovoid regions sharing the same top electrode. Inset: Side-on view of the nanovoid cell. (b) Scanning electron microscope images of polymer-coated nanovoids and (c) polymer-coated nanovoids with evaporated Al top contact.

materials in a range of geometries [3], showing enhanced performance arising from the resonant scattering of light into photoactive layers. Recently, propagating surface plasmon modes arising from structured metal surfaces [4–6], gratings [4–6] and hole-arrays [13–16] have been investigated for photovoltaic enhancement, showing increased absorption predominantly due to the coupling of light into waveguide modes within the photovoltaic layers [1, 7, 19]. Nanovoid plasmonic enhancement is distinct from both nanoparticle and surface-scattering plasmonics in that strong fields are supported *within* the nanovoid structure. Light incident upon noble metal nanovoids excites localized surface plasmons which we have extensively studied [17, 18] as well as their application in surface enhanced Raman scattering [20]. Here we harness these localized field enhancements in addition to scattering from the nanovoid lattice to improve solar cell performance. Our novel [21] nanovoid cell geometry (Fig. 1) simultaneously increases absorption and harnesses the plasmonic substrate for electrical contact.

As with all rear-surface plasmonic designs, the absorption of short wavelengths is not compromised before reaching the resonant plasmonic structures [19, 22], and enhancement can be achieved in concert with top-surface light trapping techniques, including that of plasmonic nanoparticles. Our nanovoid structures additionally display strong dewetting properties [23] similar to recently reported self-cleaning nanodome cells [5], and have significant capacity for omnidirectionality in absorption [24].

2. Methods

Metallic nanovoids are formed by electrochemical deposition through a template of close-packed self-assembled latex spheres [25]. The spheres are subsequently dissolved leaving an ordered array of sphere segment nanovoids. Nanovoids can be produced controllably without top-down lithography and can be tuned simply through their height and diameter. Here we fabricate hemispherical silver nanovoids of 200 nm radius and height. A 115 nm hole-conducting PEDOT:PSS layer is spun on top of the hemispherical nanovoids at 1500 rpm for 1 min with 0.3% (FSO Zonyl) surfactant and annealed at 180°C for 30 min under nitrogen. An organic photovoltaic polymer blend of regioregular poly(3-hexylthiophene) (P3HT, Merck) and phenyl-C60-butyric acid methyl ester (PCBM, Nano-C) is dissolved in ratio 1:0.8 at a concentration of 20 mg/mL in dichlorobenzene. The solution is spun at 1000 rpm for 1 min and annealed at 115°C for 15 min under nitrogen to form a 90 nm active layer. Finally, 15 nm of aluminium is thermally evaporated through a mask to conformally pattern the semi-transparent top contact (Fig. 1c) and the device encapsulated with a thin glass coverslip.

3. Results

3.1. Angularly-resolved reflectance

Angularly-resolved reflectance of (a) polymer on flat silver, (b) uncoated silver nanovoids, and (c) polymer-coated nanovoids (Fig. 2) provides direct access to the energy-momentum dispersion relation of plasmonic resonances. Measurements are taken using a supercontinuum white-light laser with wavelength range 500 – 1500 nm, and are normalized to flat silver.

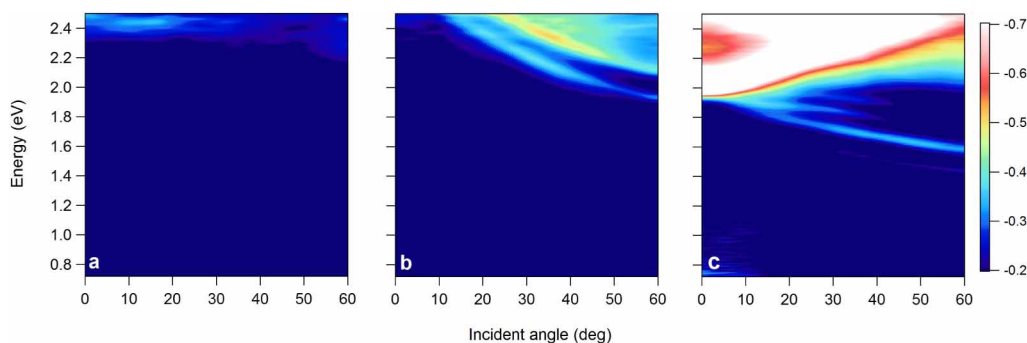


Fig. 2. Angularly-resolved reflectance of (a) polymers on flat silver, (b) bare silver nanovoids, and (c) polymers on silver nanovoids. Colour scale is $\log(\text{reflectance})$ with blue indicating high reflectance and red-white indicating low reflectance.

The angularly-independent absorption of P3HT:PCBM polymer blends on flat silver (Fig. 2a) shows the typical onset of absorption from 2.2 eV. For uncoated silver nanovoids (Fig. 2b) propagating Bragg surface plasmon modes are seen, coupled via the ordered hexagonal lattice of the nanovoid substrate [17, 18]. These provide a similar absorption enhancement mechanism to the back-surface-grating-like structures reported previously [1, 5, 8, 9, 12, 15]. These Bragg modes for the silver/air interface red-shift in the polymer-coated silver nanovoids (Fig. 2c) due to the increased refractive index of the polymer relative to air, appearing at 2 eV.

For a silver nanovoid/air interface, *localized* plasmon modes only appear above 3 eV. These also red-shift when polymer layers ($n=1.59$) encapsulates the void, as observed in our theoretical simulations (Fig. 3a). This red-shift is sensitive to the polymer thickness inside the void and supports the successful conformal coating of the 115 nm PEDOT:PSS and 90 nm

P3HT:PCBM layers (Fig. 1b). Enhanced absorption is observed over a wide range of incident angles, favourable for real environments with significant diffuse sunlight [24].

3.2. Theoretical simulation

To model nanovoid plasmonic effects we use a boundary element model for axially-symmetric structures that expresses the field in terms of charges and currents on the structure surface [26]. Decomposing the field in terms of each azimuthal component allows a computationally efficient method for solving cylindrically symmetric structures. Modelled void structures are embedded in a weighted dielectric comprising the polymer and Al layers of the experimental cell structure, with refractive indices from [27–29]. Incident light is TM polarised, and dielectric structure is modelled as isotropic (including 10% birefringence does not significantly change our results). Localized (*ie.* non-dispersive) Mie plasmons within the cavity are seen above 2 eV, with specific momentum matching required for the different modes [17], agreeing well with experimental results (Fig. 2). Energies beyond 2.5 eV are included in the theoretical analysis to examine the available range of $|E|^2$ field spatial variation within the nanovoid geometry.

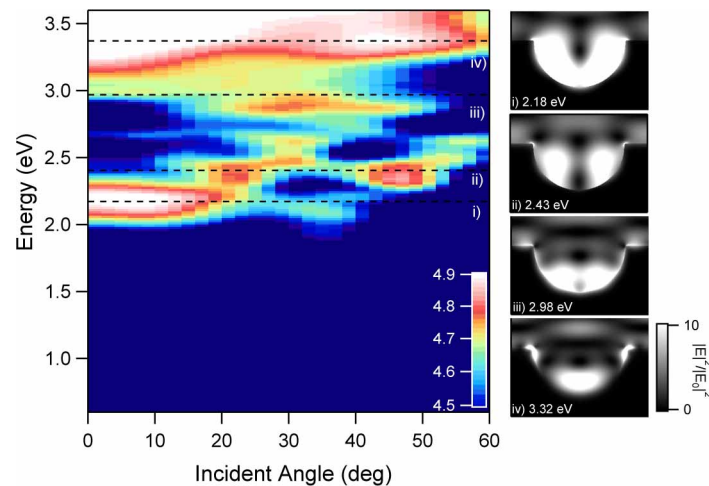


Fig. 3. Boundary element simulations of angularly resolved absorption of a silver nanovoid structure embedded in solar cell materials, details in text. Colour scale is log of absorption cross section (nm^2). (i-iv), Electric field intensity profiles at normal incidence.

Simulations of the $|E|^2$ field intensity at these resonances (Fig. 3) demonstrate the significant field enhancements within the void structure. It is these regions of concentrated field that elicit enhanced absorption within the polymer-coated nanovoids. Different spatial distributions for higher energy localized modes are observed within the void geometry [17]. This spatial tuning suggests a first step towards plasmonic enhancement for third-generation thin-film PV devices, with nano-cavity plasmonic resonances at different wavelengths tailored to selectively enhance absorption in matched materials at targeted device locations.

3.3. Photocurrent measurements

For the uncapped nanovoid/polymer structures a peak in absorption is observed at 590 nm (Fig. 4a), rising again towards 500 nm. These absorption enhancements correspond to the localized plasmon resonances near 2.2 eV and 2.5 eV. The peak at 590 nm is due to a mixed mode [18] between the localized mode and the propagating surface plasmons seen in Fig. 2c. Transfer

matrix simulations (green lines) of the planar devices (with P3HT:PCBM optical constants from Hoppe *et al.* [27]) match the data well.

The enhanced optical absorption in the nanovoid geometry improves the PV performance. External quantum efficiency (EQE) at zero bias and a reverse bias of -1 V are measured with a monochromated xenon lamp. The measurements at reverse bias extract nearly all of the light-generated carriers, separating effects of absorption enhancement and carrier transport. Nanovoid and flat cell measurements are taken from the *same* cell pixel containing separate nanovoid and flat sections of the silver substrate (Fig. 1b). The measurements are representative across a range of cell pixels and cell batches.

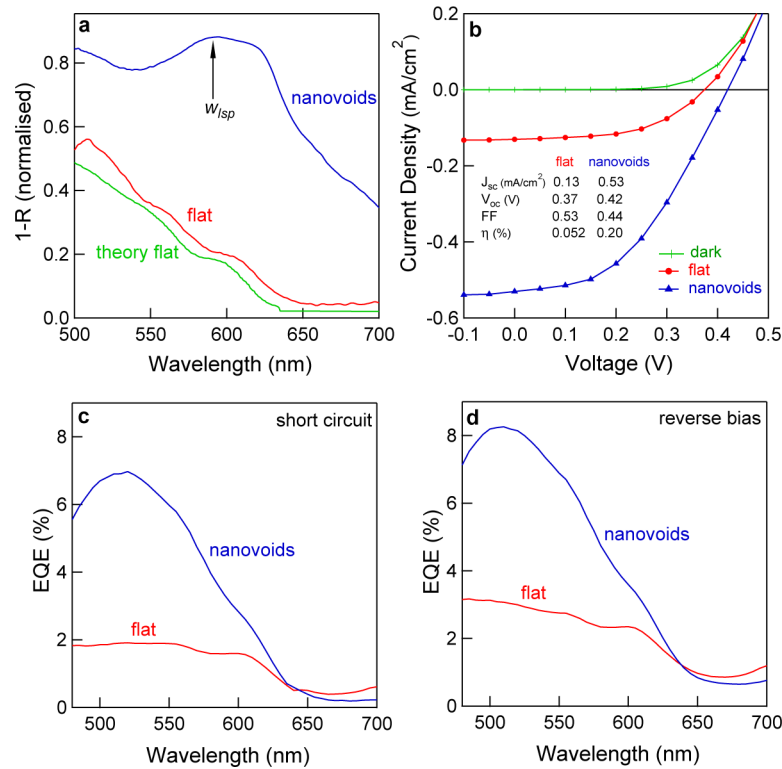


Fig. 4. **a**, Extinction spectra, $A(\lambda) = 1 - R$, at normal incidence for polymer on silver nanovoids (measured, blue) and flat silver (measured, red) with transfer matrix simulations for the planar structures shown in green. **b**, J-V curves under xenon lamp illumination comparing nanovoid cells to flat cells. The dark J-V curve is common to both. **c**, External quantum efficiency (EQE) at zero bias and reverse bias -1 V (**d**) of nanovoid cells vs. flat cells.

A strong peak at 520 nm in charge-carrier generation is observed for the nanovoid cell compared to the planar cell (Fig. 4c). The position of the peak corresponds well to the expected localized plasmon resonance of the polymer-coated silver nanovoid, with the variation from Fig. 4a due to slight variations in polymer coating thickness between samples used for spectral measurement and encapsulated cells with Al top-contacts used for EQE. Additional effects are expected due to spatial variation of photo-injection in different locations at different wavelengths, currently under investigation. We find that plasmonic field enhancements for the Ag nanovoid/organic semiconductor system contribute directly to enhanced photocurrent with

proportionally higher absorption in the semiconductor than in the silver, highlighting the importance of active material absorption for plasmonic cell design [9]. Little difference is found between EQE at short circuit (Fig. 4c) and at -1 V (Fig. 4d) measurements, indicating that the significant differences between nanovoid and planar cells are due to light absorption and not charge-carrier extraction.

The nanovoid cell shows higher EQE across large spectral bandwidths from $\lambda = 450 - 650\text{ nm}$. The slight improvement in planar device performance for $\lambda = 650\text{ nm}$ is due to the Fabry-Pérot mode between the flat Ag and Al layers.

Overall efficiencies are limited by the excessive reflectivity of the 15 nm Al top contact, with a maximum EQE of 7% from all devices. Transfer matrix simulations indicate $< 8\%$ of incident light from $400 - 800\text{ nm}$ is transmitted through the Al so that $> 90\%$ of visible light is reflected, implying effective internal efficiencies are really in excess of 50% . In addition, layer thicknesses of the active polymer and PEDOT:PSS have not been optimised for absorption and carrier extraction. The flatter EQE of the planar cells from $\lambda = 460 - 550\text{ nm}$ compared to Kim *et al.* [30] is also due to these microcavity spectral effects, as well as contributions from wavelength dependent carrier-extraction (seen from the EQE at -1 V). Despite this, we clearly show here that absorption is enhanced over $460 - 650\text{ nm}$ for a nanovoid cell compared to an identically prepared flat cell sharing the same electrode.

4. Discussion

Three key features give rise to absorption differences between a flat cell and a nanovoid cell: i) localized and surface plasmon coupling, ii) PV material volume and morphology, and iii) light scattering from the textured back surface. Fabricating cells within sphere segment voids increases the Ag substrate area. Replacing flat with textured reflecting substrates of nanovoids increases the average optical path within the cell.

Increased active semiconductor area and enhanced scattering from the textured surface are significant advantages to the nanovoid geometry, increasing efficiency across the spectrum. Neither, however can account for the strong increase in EQE at 520 nm . We thus explain this enhancement by localized plasmonic resonances of the polymer-coated silver nanovoids, eliciting higher absorption within active semiconductor regions.

The overall enhancement in charge-carrier generation for the nanovoid cell compared to flat cells is expressed in the short-circuit current density (J_{SC}) of the J-V curves (Fig. 4b, dark J-V curve common to both) under white light (Newport Xenon Lamp 96000, AM1.5G spectral mismatch factor 2.0) at an intensity equivalent to 0.5 suns at AM1.5G after spectral mismatch correction. A sharp increase in J_{SC} from 0.13 to 0.53 mA/cm^2 is observed in the nanovoid cell, with a corresponding increase in open circuit voltage (V_{OC}) from 370 mV to 420 mV due to the standard solar cell equation. The fill factor of the nanovoid cell is slightly decreased from 0.53 to 0.44 for the nanovoid cell, possibly due to the increased resistance of the now textured aluminium top-contact. Overall, nanovoid cells show four-fold enhancement in total cell efficiency from 0.052% to 0.20% . These organic plasmonic solar cells we refer to as orgasmonic when showing enhancement. Absolute efficiency values are currently limited by the significant reflection from the 15 nm Al top contact. This can be ameliorated in next generation designs in progress - as typical for the first demonstration of a new physical phenomena further optimisation is required to achieve technology-compatible results, however we find clear evidence for plasmonic enhancements to photovoltaics from this localised plasmon configuration.

5. Conclusions

In conclusion, we have fabricated solar cells *within* plasmonically-resonant nanostructures to enhance absorption, demonstrating a new class of plasmonic photovoltaic enhancement avail-

able to all solar cell materials. Significant PV enhancement is observed in our nanovoid organic solar cells compared to identically-prepared flat cells, with a four-fold enhancement of overall power conversion efficiency, due largely to an increase in J_{SC} . This enhancement in nanovoid cells is primarily due to strong localized plasmon resonances of the nanovoid geometry. Theoretical modelling suggests future third-generation plasmonic photovoltaic devices that utilise the spatial distribution of field enhancements within plasmonic nanostructures. Our results indicate the significant potential for enhanced photovoltaics utilising localized plasmon resonances within nanostructured geometries.

Acknowledgments

We gratefully acknowledge the UK Engineering and Physical Sciences Research Council (EPSRC) grants EP/C511786/1, EP/F059396/1, EP/E040241. The authors thank Hang Zhou for assistance with solar simulator measurements. N. N. L. acknowledges the support of the Gates Cambridge Scholarship.